Reynolds number similarity of orthogonal decomposition of the outer layer of turbulent wall flow

Z.-C. Liu [a),b)], R. J. Adrian [a)], T. J. Hanratty [b)]
[a)] *Department of Theoretical and Applied Mechanics*
[b)] *Department of Chemical Engineering*
University of Illinois
Urbana, Illinois 61801

Experimental evidence is presented to show that in the outer region of wall-bounded turbulent flow both the eigenfunctions and the eigenvalue spectra of the one-dimensional proper orthogonal decomposition have forms that are independent of Reynolds number when scaled by the wall friction velocity and the outer length scale.

The proper orthogonal decomposition of Lumley[1,2] defines a deterministic set of orthonormal basis functions for a given random process. The set is optimal in the sense that expansion in terms of these basis functions converges faster than expansion in terms of any other set of basis functions. The topic has been reviewed recently by Berkooz, Holmes and Lumley[3]. When applied to turbulent velocity fields, the basis functions are the eigenfunctions of a Fredholm integral equation whose kernal is the two-point correlation function of the random velocity field. If the turbulence is statistically homogeneous, the eigenfunctions reduce to the trigonometric functions and POD becomes conventional Fourier analysis. If, however, the turbulence is statistically inhomogeneous, POD defines a non-trigonometric set of eigenfunctions whose structure reflects the physics of the inhomogeneity, as imbedded in the structure of the two-point correlation function.

While many of the more attractive properties of POD derive from the fact that it is based on correlation functions that contain important information about the physics of a particular flow, the need to input the correlation functions also makes implementation of the POD difficult because the correlation functions are seldom available, especially for inhomogeneous, anisotropic flow. There are two scenarios in which this difficulty is ameliorated.

First, if the eigenfunctions of the POD are sufficiently insensitive to the form of the correlation function, it may be satisfactory to use approximate correlation functions, or approximate eigenfunctions which, though incorrect, capture at least some of the important aspects of the flow inhomogeneity. The work of Sirovich and Rodriguez[4] and Rodriguez and Sirovich[5] with the POD of the Ginzburg-Landau equation suggests that this may be

possible. They considered expansion of the solution at one value of a Reynolds number-like parameter that was based on eigenfunctions computed from the correlation function for a value of the parameter that differed by a factor of three. The eigenfunctions for the first Reynolds number, were effectively sub-optimal models of the eigenfunctions for the second Reynolds number. Expansion in terms of the sub-optimal eigenfunctions converged almost as fast as the optimal expansion.

Second, if the eigenfunctions possess a property of universality similar, for example, to that of the celebrated law of the wall or the spectral similarity laws of turbulence, then it would be possible to use a single set of eigenfunctions to represent flows at many Reynolds numbers. The work of Chambers, et al.[6] explored this possibility by using Burger's model on a unit interval with the random forcing to create a temporally stationary, spatially inhomogeneous process possessing a two-scale boundary layer character at the end-points of the interval. They showed that the POD eigenfunctions in the inhomogeneous spatial variable were similar over a range of Reynolds numbers if they were scaled on outer variables . It was conjectured that the POD of real turbulence might also obey such a generalized law of Reynolds number similarity .

In this letter, we describe results that indicate that the one-dimensional eigenfunctions of three dimensional wall turbulence exhibit similarity in the form of Reynolds number independence of the outer regions of both the eigenfunctions and the spectrum of eigenvalues, when scaled properly with outer variables. Demonstration of this property is based on experiments conducted in plane, fully developed turbulent channel flow at two Reynolds numbers, $Re_h=U_B h/\nu$ =5,378 and 29,935, where U_b is the bulk velocity, $2h$ is the total channel height, and ν is the kinematic viscosity. These two Reynolds numbers provide a range of variation (5.5:1) adequate to make a credible test of Reynolds number invariance while keeping the lower Reynolds number high enough to avoid some of the peculiarities of very low Reynolds number turbulence, and the upper Reynolds number low enough to maintain reasonable spatial resolution of the outer scales of motion.

The rectangular channel cross-section is 609.6 mm wide by $2h$=48.75 mm high and the water flow is fully developed. Conventional coordinates are used with $(u,v,w)=(u_1,u_2,u_3)$ referred to (x,y,z) coordinates in the streamwise , cross-stream and spanwise directions, respectively. Turbulent flow in this channel has been documented previously by LDV studies[7,8], and comparisons of the time averaged moments of the u- and v- fluctuations through fourth order at Re_h= 2,777 and 18,000 agree well with the channel flow results of other investigators. Pertinent properties of the flows are listed in Table 1, wherein u* is the friction velocity found by using direct measurements of the bulk velocity and Dean's correlation of the friction coeffeicient as explained in Ref. 8.

Table 1. Properties of channel flows

$U_b h/\nu$	U_b (mm/s)	u^* (mm/s)	ν/u^* (mm)	Δx^+	Δy^+	Δz^+
5,378	212	12.4	0.0775	20.6	10.3	10.3
29,935	1,074	50.7	0.0172	93.0	46.5	46.5

$\Delta x/h$	$\Delta y/h$	$\Delta z/h$
0.065	0.032	0.032

Measurement of the u- and v-components of the velocity field in an x-y plane extending completely across the channel are made by planar light sheet particle image velocimetry. The techniques have been described previously in Liu, et al.[9] Scattering particles were 9.5 micron nominal mean diameter aluminum oxide particles illuminated by two 2J ruby laser pulses. The time between pulses was adjusted to produce an average displacement of approximately 0.25 mm, thereby satisfying the "one-quarter rule" for double-pulsed autocorrelation PIV[10]. Double pulsed particle images over a field of view that spanned the channel and covered approximately 120mm in the streamwise direction were recorded on 4" x 5" Kodak 4415 film using a single lens scientific camera with magnification M=0.97 and f/9 Schneider lens. The angular field-of-view was small enough to limit errors due to the perspective effect [11] to a maximum value of 1.7 % of the bulk velocity over the entire field of of view. Photographs were interrogated automatically by direct spatial correlation of the images in small interrogation spots using the PIV interrogation system described in Ref. 12.

The measurements so obtained represent the Eulerian velocity averaged over a measurement volume defined by the virtual intersection of the interrogation spot with the laser light sheet[13]. The interrogation spot dimensions were chosen to produce measurement volumes with dimensions Δx= 1.6mm, Δy=0.8 mm and Δz= 0.8mm in the fluid. The dimensions in Table 1 are given in terms of viscous wall unit and relative to the channel height. At the lower Reynolds number the spatial resolution is comparable to that achieved in direct numerical simulations,but at the higher Reynolds number the measurement from each independent (e.g. non-overlapping) interrogation spot represents an average over a significant range of small scales. For example, the resolution in the y-direction Δy^+= 46.5 is inadequate to resolve the buffer layer, but relative to the outer length scale h, the resolution $\Delta y/h$=0.032 is capable of resolving POD modes in the y-direction up to mode numbers of order 15, considerably beyond the mode number considered here. Interrogation

was performed on a uniform, rectangular grid of points with spacing 1.2mm in the x- and 0.6mm in the y-- directions (25% overlap of interrogation spots).

Statistical quantities are computed by averaging along line of constant y in the data from each PIV photograph, and averaging the line averages over ensembles of 60-80 photographs for each Reynolds number. Turbulent fluctuation data is defined by subtracting the ensemble mean velocity from the total velocity field of each photograph. Profiles of the mean streamwise velocity, the *rms* streamwise and cross-stream turbulent velocities and the turbulent Reynolds shear stress all compare well with accepted data.

The two-point spatial correlation function with one-dimensional separation in the y-direction

$$R_{ij}(y, y') = < u_i(x,y,z,t)u_j(x,y',z,t) >, \qquad i,j=u,v \qquad (1)$$

is computed from the ensemble of PIV photographs in a similar manner. To illustrate the character of the PIV correlation data normalized correlation coefficients

$$R_{uu}(y,y')/ [R_{uu}(y,y)\ R_{uu}(y,'y')\ ]^{1/2}$$

are plotted in Fig. 1 for three different values of y. The complete data set for one Reynolds number consists of 75 such curves , one for each y-location across the width of the channel. Similar data are available for R_{vv}, R_{uv} and R_{vu}. Near the top of the channel laser flare made PIV measurements unreliable.

The one- dimensional POD is found by solving the eigenvalue problem

$$\int_0^h R_{ij}(y,y')\varphi_j^{(n)}(y')dy' = \lambda_n \varphi_i^{(n)}(y) \qquad (2)$$

The decomposition is performed on the half-channel domain $(0,h)$, principally to avoid the region of missing correlation data on the upper wall, but also because the half-channel velocity profile corresponds more closely to a boundary layer than the full channel profile. Integration is done using the trapezoidal rule and the IMSL eigenvalue routine DEVCHF . Computations are carried out up to order n=10. Beyond that order statistical sampling errors in the measurement of R_{ij} render the eigenvalue computation unreliable.

The scales of motion in the outer layer of the channel flow are taken to be h and u^*. In terms of these scales the non-dimensional length is y/h , the non dimensional eigenvalue is $\lambda/u^{*2}h$, and the non-dimensional eigenfunctions are $h^{1/2}\varphi_i^{(n)}$. The factor of

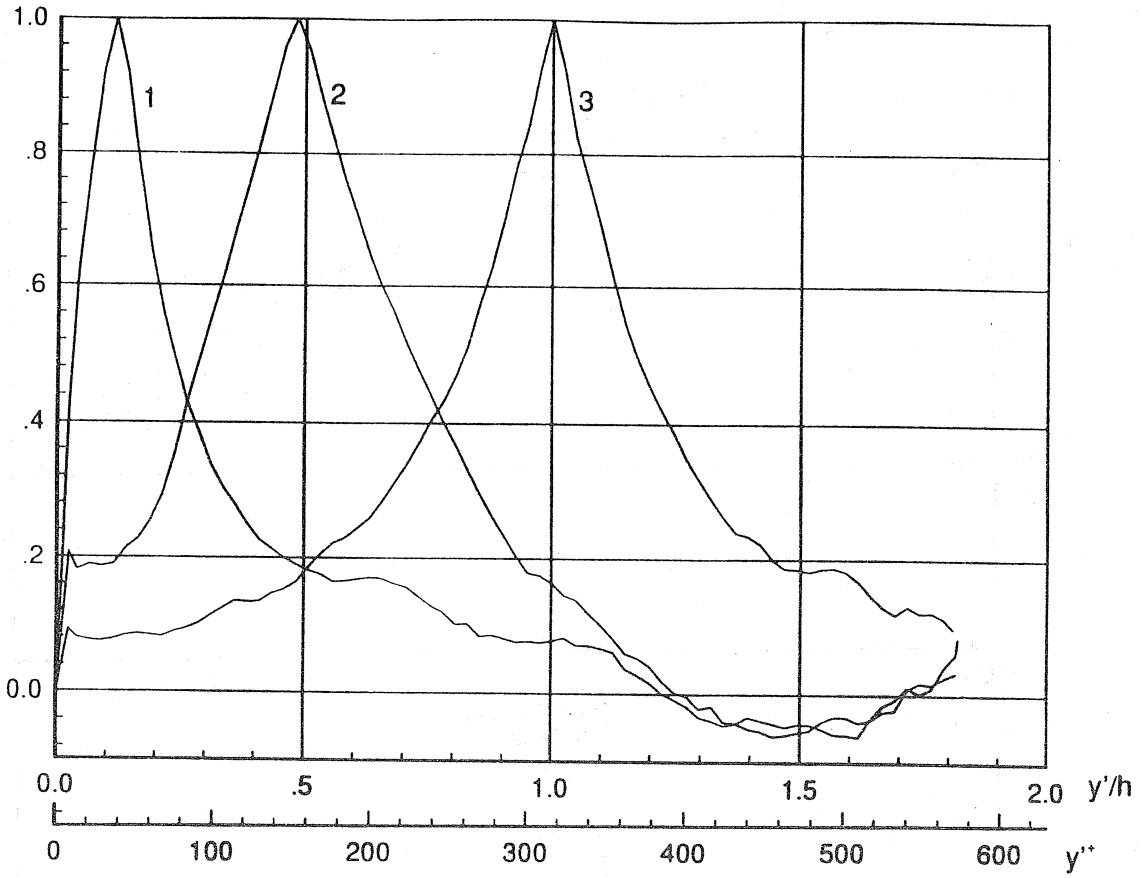

FIG. 1.Two-point correlation functions $R_{un}(y,y')/u_{rms}(y)\,u_{rms}(y')$ at Re_h = 5,378. The fixed points are at y/h = 0.114, 0.476, and 0.50, corresponding to the top of the buffer layer, the top of the log-layer, and the centerline of the channel.

$h^{1/2}$ is determined by the condition of orthogonality[6]

$$\int_0^h \varphi^{(m)}(y)\varphi^{(n)}(y)dy = \delta_{mn}, \tag{3}$$

The scaling of $\varphi_i^{(n)}$ is independent of u^* because Eq.(2) is homogeneous in $\varphi_i^{(n)}$, and it therefore imposes no dimension on the eigenfunction.

Non-dimensional eigenfunctions computed from the correlation data at Re_h= 5,378 and 29,935 are compared in Fig. 2.(Scaling by $h^{1/2}$ is optional in Fig. 2 because the channel height was not varied in the experiments. It is introduced solely for consistency.) Eigenfunctions of the u- and v- components are shown through order four . The u-eigenfunctions are clearly dependent on the Reynolds number in the region adjacent to thewall where the inner wall layer significantly retards the streamwise motion. This region extends up to approximately y/h = 0.2 depending upon the Reynolds number. Above the

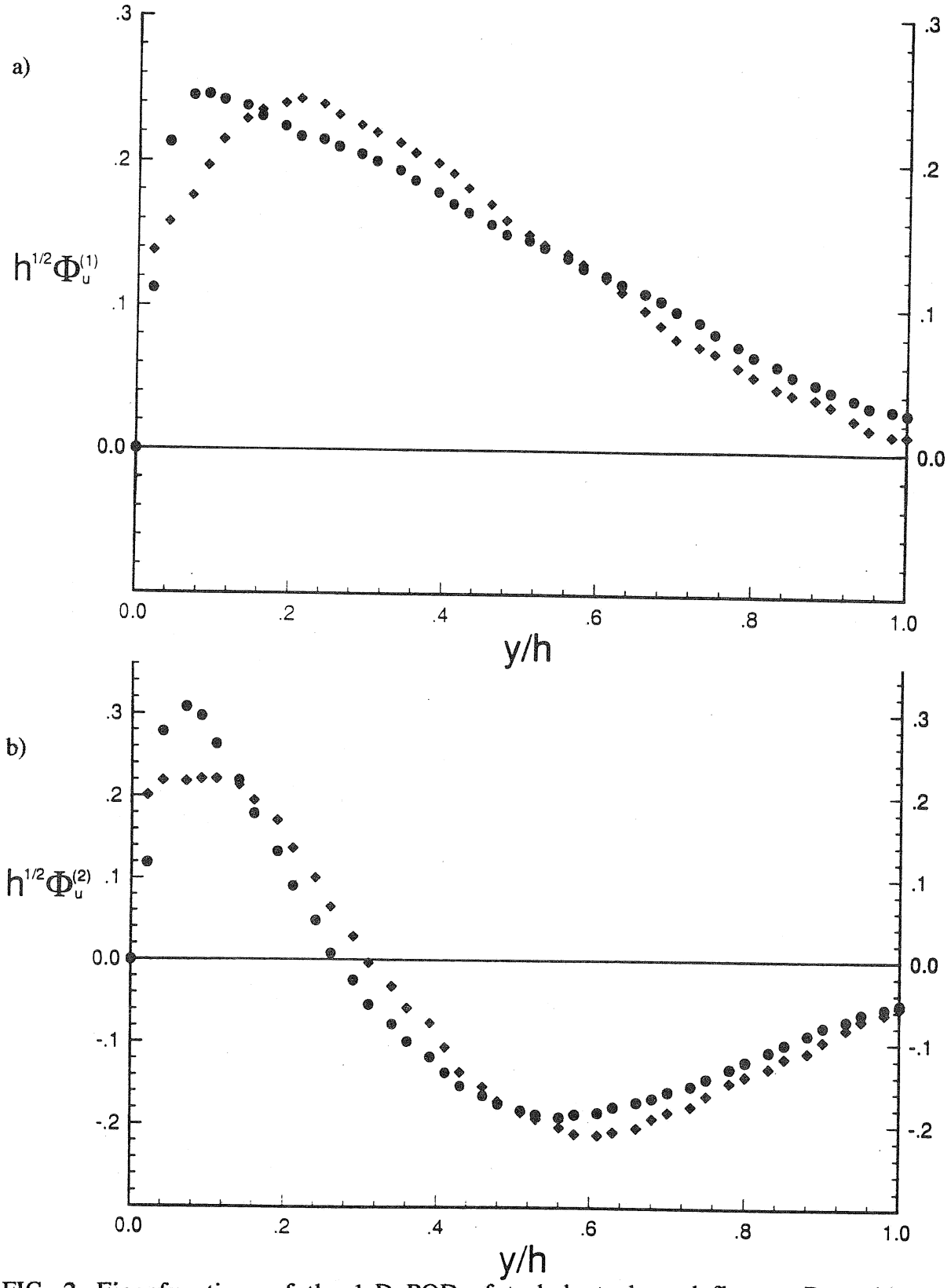

FIG. 2. Eigenfunctions of the 1-D POD of turbulent channel flow at Reynolds number=5,378 (circles), 29,935 (squares). The decomposition domain is $0 \le y \le h$. (a), (b), (c), and (d) are the eigenfunctions of the u- component, n= 1, 2, 3,4; (e), (f), (g), and (h) are the eigenfunctions of the v- component, n=1, 2, 3,4.

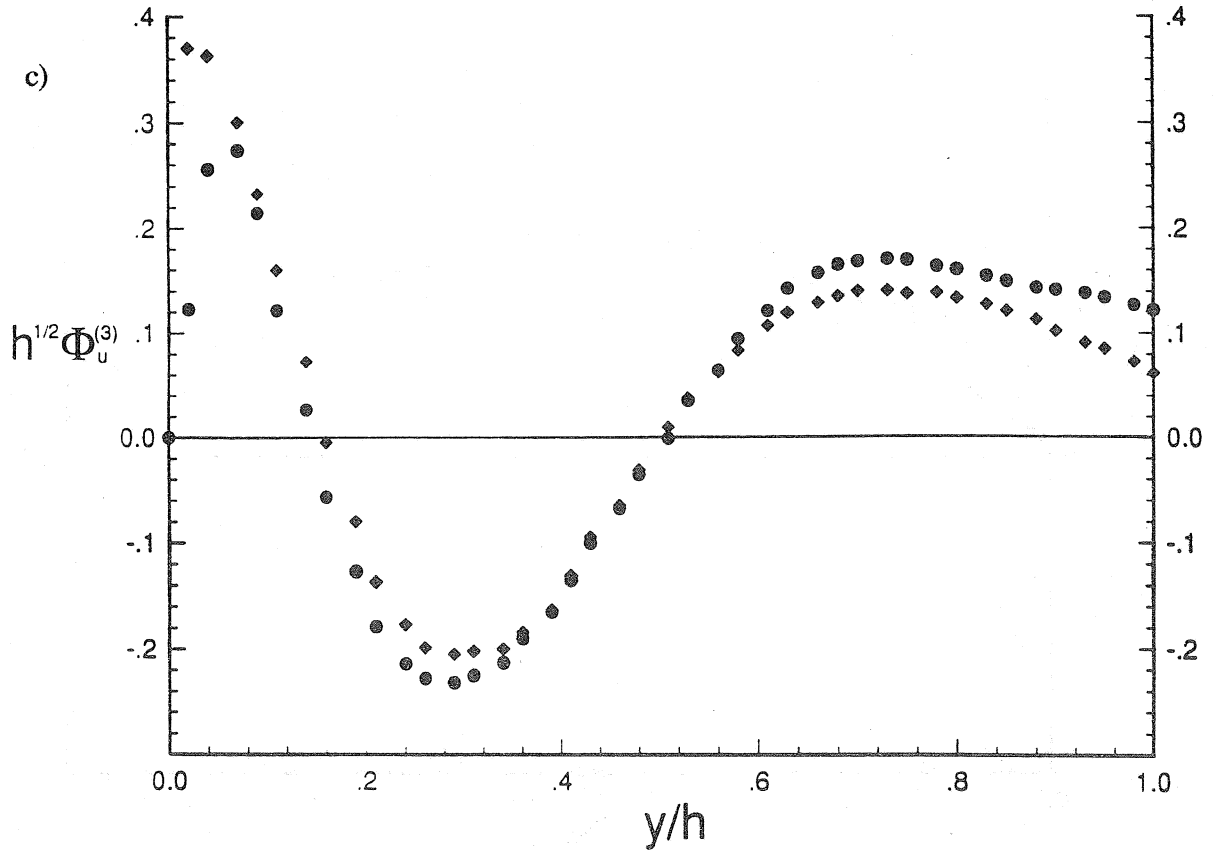

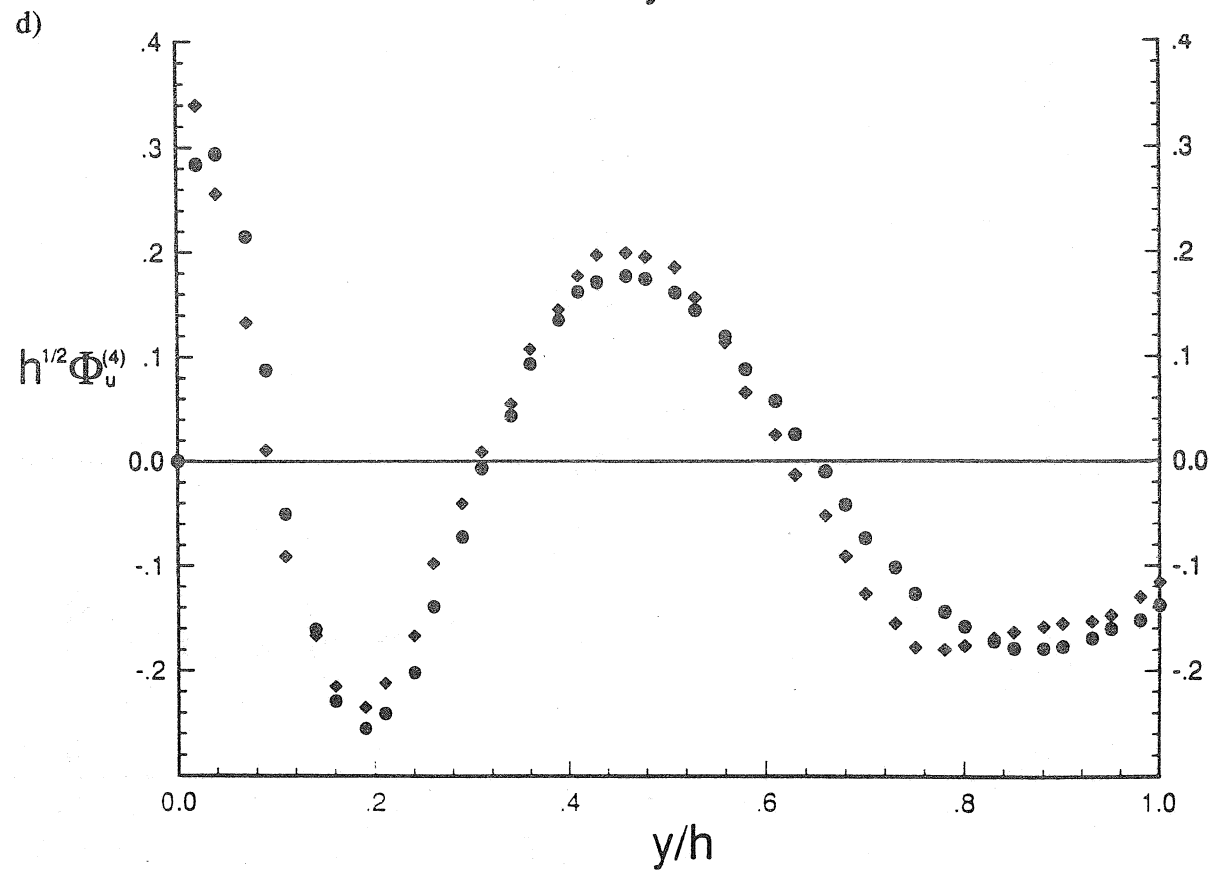

FIG. 2. Continued

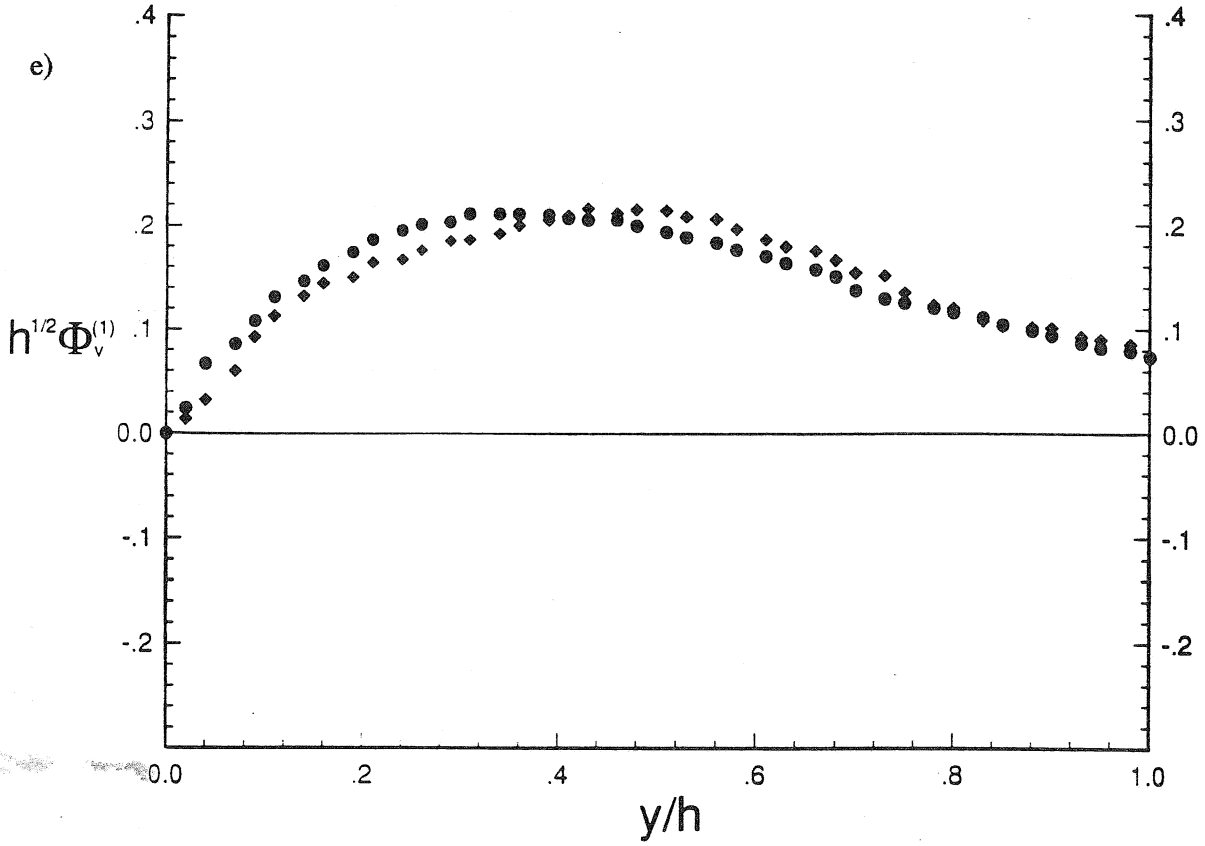

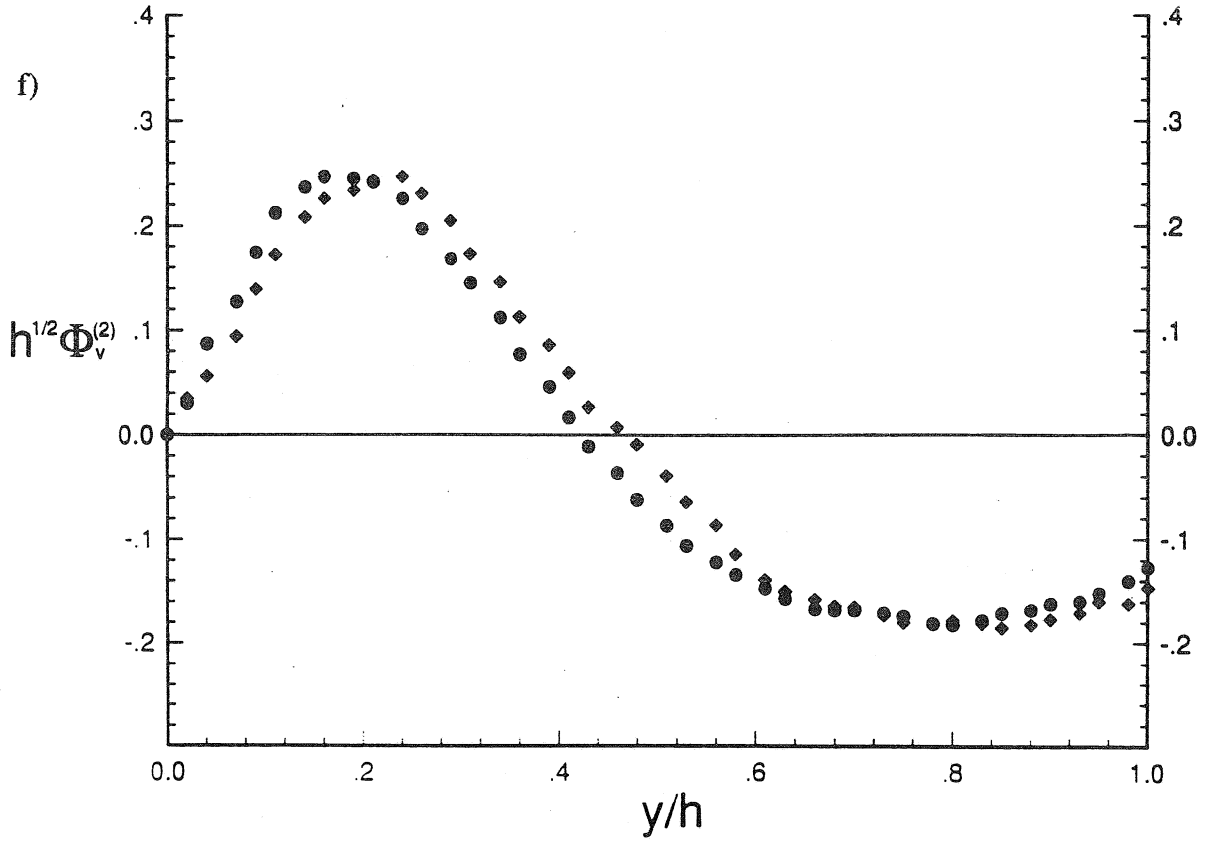

FIG. 2. Continued

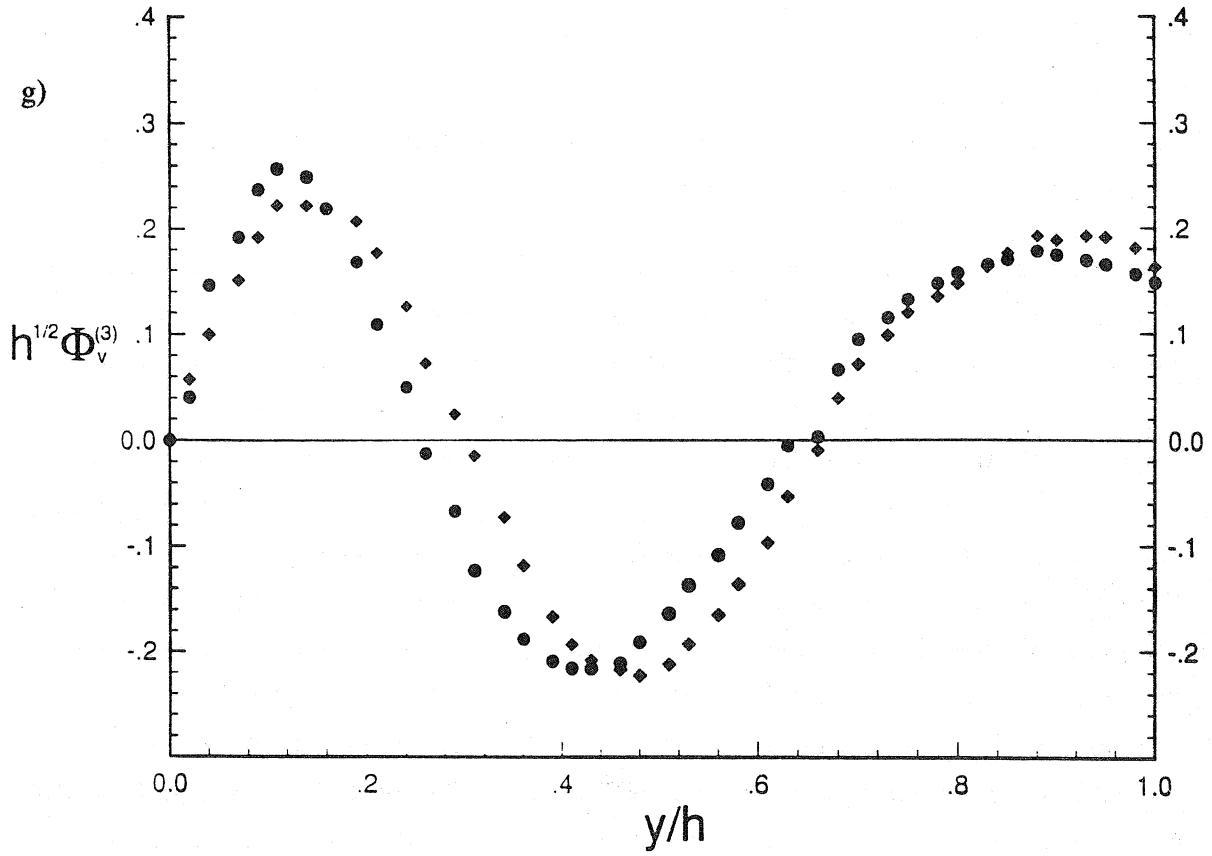

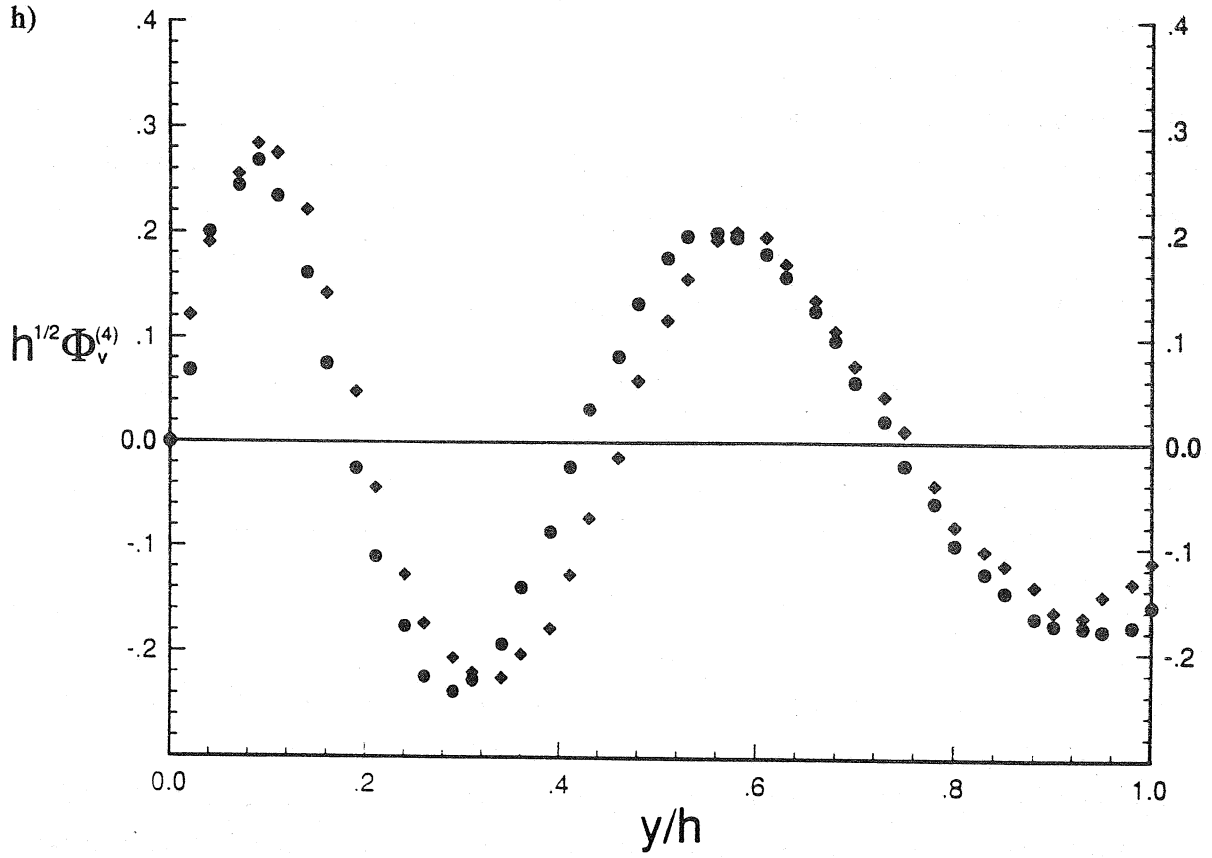

FIG. 2. Continued

wall layer the eigenfunctions of any order are remarkably similar at both Reynolds numbers. Small differences that do appear in the comparisons are within the estimated sampling error in the measurements of R_{ij}

The non-dimensional eigenvalue spectra of the POD for both Reynolds numbers are shown in Fig. 3. Since the spectra are monotonic, the mode number n of the energy-ordered eigenvalues is related simply to the *sequency*, which is defined as the number of zero crossings of the associated eigenfunction in the interior of the domain $(0,h)$. By inspection of Fig. 2 it is clear that the mode number is equal to the number of half-cycles in the length h. If the process was homogeneous, the eigenfunctions would be trigonometric, and the lengths of the cycles would be uniform. Since it is inhomogeneous, the lengths of the cycles vary, increasing with distance from the wall. Evenso, the analogy with trigonometric functions is clear, and it is natural to interpret n as the number of half-wavelengths in h. To within a factor of 2π this is analogous to the usual trigonometric wavenumber k made dimensionless by the outer scale of length, h.. Thus, Fig. 3 represents the outer scaling of the eigenvalue spectrum. The similarity of the spectra at the different Reynolds numbers is evident. It was shown earlier that spectra of Burgers equation which were similar at low mode numbers still depended upon the Reynolds number at higher values of the mode number, presumably because of the increased significance of viscosity at small scales. The spectra for the channel show no such differences, suggesting that the mode numbers attainable from the experimental data are not high enough to reveal clearly the effects of viscosity on the spectra. On physical grounds and by analogy with the similarity behavior of power spectra of homogeneous turbulence we should not expect the Reynolds number similarity to extend over all mode numbers.

The foregoing results lead us to state the following principle of large scale similarity of the POD eigenfunctions for a fully turbulent process: *In the region outside of the wall layer and in the range of sequencies where the wavelength is large compared to the wall layer viscous length scale, both the eigenfunctions and the spectrum of the eigenvalues when scaled by outer layer variables are independent of the Reynolds number for sufficiently large Reynolds number.*

It is of considerable interest to ask if the similarity principle can be extended from channel flow to a broader class of turbulent wall flows. Some indication that such generalization is possible is obtained by comparing the POD results of Lu and Smith[14] for a boundary layer to the present results for channel flow. The Reynolds numbers of these flows based on the centerline velocity and the momentum thickness of the mean velocity

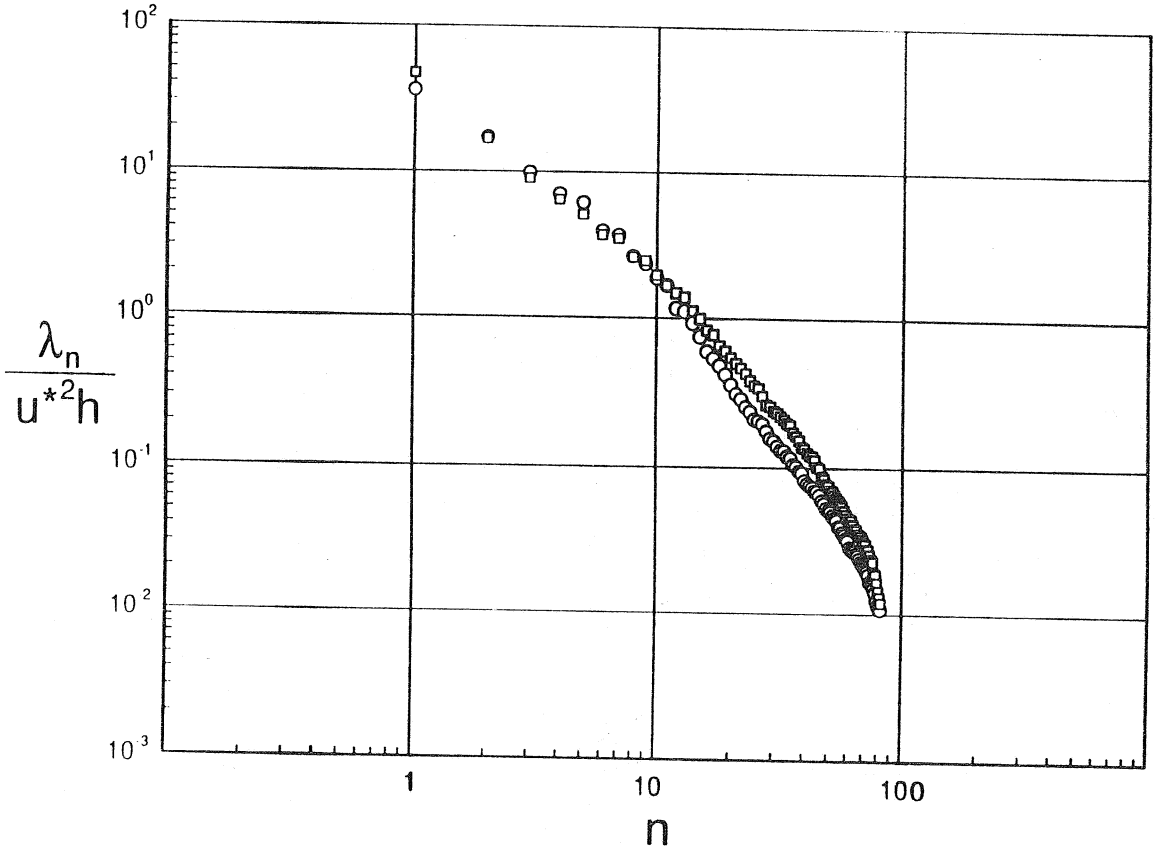

FIG. 3. Eigenvalue spectra of the 1-D POD of turbulent channel flow at Re_h = 5,378 (circles), 29,935 (squares). The decomposition domain is $0 \leq y \leq h$.

profile are 1120 for the boundary layer and 543 for the Re_h = 5,378 channel flow. For purposes of comparison the eigenvalue problem has been recomputed on a domain extending from the wall up to y^+= 130, the upper limit of Lu and Smith's data. The non-dimensional eigenvalue spectra in Fig. 4 agree very well. The eigenfunctions display some differences in the amplitudes of their oscillations, but these may be to due to noise in the correlation data. A more fundamental property of the eigenfunctions, the locations of the zeroes, behaves almost identically for both flows. The patterns of the locations of the zeroes of each of the modal orders (see the inset of Fig. 4) are remarkably similar . While universality of the outer law for the POD will require further proof, the similarity between the boundary layer flow and the channel flow is very suggestive.

In summary, in the outer region of wall turbulence the eigenfunctions and eigenvalues of the POD have been shown to be similar when scaled by outer variables. The similarity extends over different Reynolds numbers and different flows. One may view this similarity as a generalization of the classical law of the wall to the POD. The similarity signifificantly simplifies the representation of turbulence by POD, and makes it feasible to apply the POD decompostion more widely.

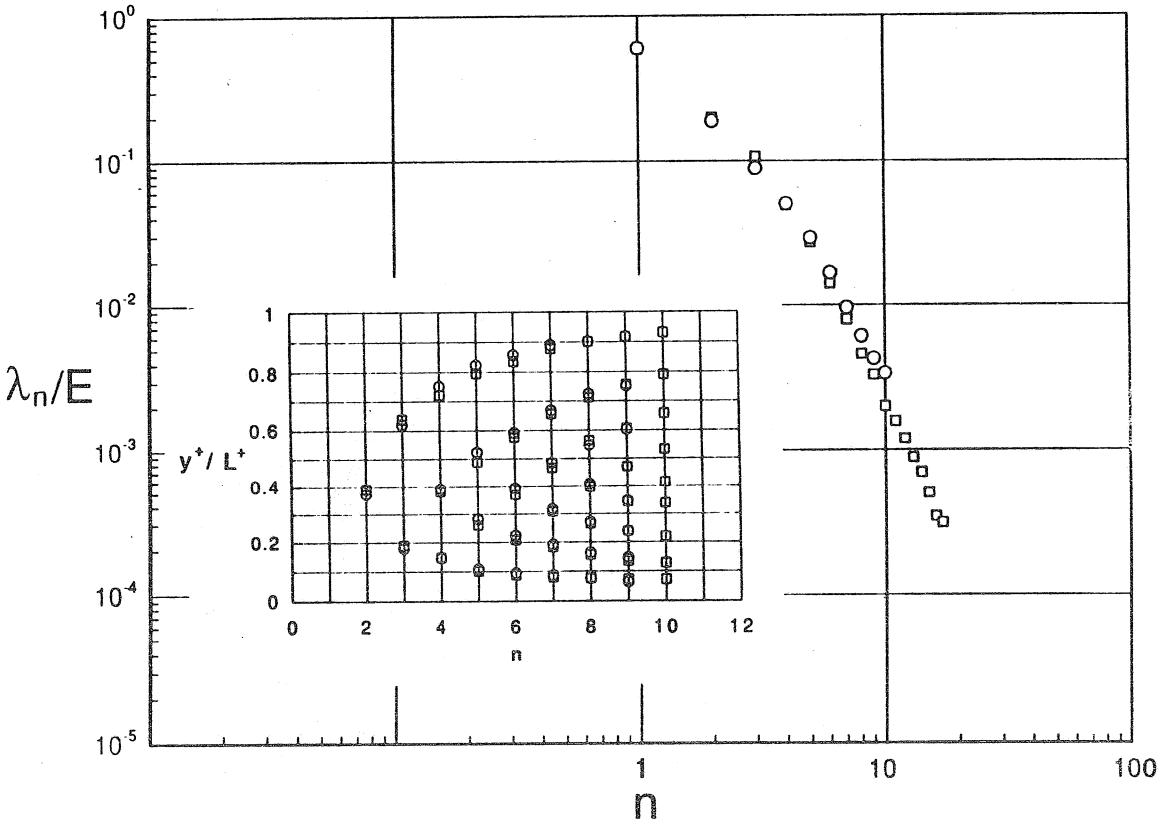

FIG. 4. Eigenvalue spectra of turbulent channel flow (squares) at Re_h = 5,378 and turbulent boundary layer (circles) at Re_θ = 1120 (Lu & Smith[14]). The domain of the decomposition is $0 < y^+ < 130$ in each case. The insert shows zero crossings of eigenfunctions up to order of 9 for the two cases. The zero locations in the inhomogeneous normal direction are normalized by $L^+=130$.

Acknowledgment

This work was supported by ONR N00014-93-1-0552, NSF CTS 92-00936 and Petroleum Res. Fund for Amer. Chem. Soc. Project #35913

References

1. Lumley, J.L. The structure of inhomogeneous turbulent flows. In *Proc. Intl. Coll. on the Fine-Scale Structure of the Atmosphere and its Influence on Radio Wave Propagation.* (Dokl. Nauk., Moscow, 1967) p.166.

2. Lumley, J.L. *Stochastic Tools in Turbulence.* (Academic,New York, 1981).

3. Berkooz, G., Holmes, P., Lumley, J.L. The proper orthogonal decomposition in the analysis of turbulent flows. In Ann. Rev. Fluid Mech. **25**, 539 (1993).

4. Sirovich, L., and Rodriguez, J. D. Coherent structures and chaos: A model problem. Phys. Lett. A **120**, 211 (1987).

5. Rodriguez, J.D., and Sirovich, L. Low dimensional dynamics for the complex

Ginsburg-Landau equation. Physica D **43**, 63 (1990).

6. Chambers, D.H., Adrian, R.J., Moin, P., Stewart, D.S., and Sung, H.J. Karhunen-Loeve expansion of Burger's model of turbulence. Phys. Fluids **31**, 2573 (1988).

7. Niederschulte, M.A. Turbulent flow through a rectangular channel. Ph.D. Thesis, (University of Illinois,Urbana, 1988).

8. Niederschulte, M.A., Adrian, R.J., Hanratty, T.J. Measurements of turbulent flow in a channel at low Reynolds numbers. Expr. Fluids **9**, 222 (1990).

9. Liu, Z.-C., Landreth, C.C., Adrian, R.J., Hanratty, T.J. High resolution measurement of turbulent structure in a channel with particle image velocimetry. Exp. Fluids **10**, 301 (1991).

10. Keane, R.D., Adrian, R.J. Optimization of particle image velocimeters. Part 1: double pulsed systems. *Meas. Sci. Technol.*, **1**, 1202 (1990).

11. Adrian, R.J. Particle-imaging techniques for experimental fluid mechanics. Ann. Rev. Fluid Mech., **23**, 261 (1991).

12. Meinhart, C.D., Prasad, A.K., Adrian, R.J. Parallel digital processor system for particle image velocimetry. Meas. Sci. Tech. **4**, 619 (1992).

13. Adrian, R.J. Statistical properties of particle image velocimetry measurements in turbulent flow. In *Laser Anemometry in Fluid Mechanics*, (Ladoan, Inst. Superior Tecnico, Lisbon, 1988) p.115 .

14. Lu, J. L. and Smith, C. R."Velocity profile reconstruction using orthogonal decomposition", Expr. Fluids **11**, 247 (1991).

List of Recent TAM Reports

No.	*Authors*	*Title*	*Date*
705	Stewart, D. S., and J. B. Bdzil	Asymptotics and multi-scale simulation in a numerical combustion laboratory	Jan. 1993
706	Hsia, K. J., Y.-B. Xin, and L. Lin	Numerical simulation of semi-crystalline nylon 6: Elastic constants of crystalline and amorphous parts	Jan. 1993
707	Hsia, K. J., and J. Q. Huang	Curvature effects on compressive failure strength of long fiber composite laminates	Jan. 1993
708	Jog, C. S., R. B. Haber, and M. P. Bendsøe	Topology design with optimized, self-adaptive materials	Mar. 1993
709	Barkey, M. E., D. F. Socie, and K. J. Hsia	A yield surface approach to the estimation of notch strains for proportional and nonproportional cyclic loading	Apr. 1993
710	Feldsien, T. M., A. D. Friend, G. S. Gehner, T. D. McCoy, K. V. Remmert, D. L. Riedl, P. L. Scheiberle, and J. W. Wu	Thirtieth student symposium on engineering mechanics, J. W. Phillips, coord.	Apr. 1993
711	Weaver, R. L.	Anderson localization in the time domain: Numerical studies of waves in two-dimensional disordered media	Apr. 1993
712	Cherukuri, H. P., and T. G. Shawki	An energy-based localization theory: Part I—Basic framework	Apr. 1993
713	Manring, N. D., and R. E. Johnson	Modeling a variable-displacement pump	June 1993
714	Birnbaum, H. K., and P. Sofronis	Hydrogen-enhanced localized plasticity—A mechanism for hydrogen-related fracture	July 1993
715	Balachandar, S., and M. R. Malik	Inviscid instability of streamwise corner flow	July 1993
716	Sofronis, P.	Linearized hydrogen elasticity	July 1993
717	Nitzsche, V. R., and K. J. Hsia	Modelling of dislocation mobility controlled brittle-to-ductile transition	July 1993
718	Hsia, K. J., and A. S. Argon	Experimental study of the mechanisms of brittle-to-ductile transition of cleavage fracture in silicon single crystals	July 1993
719	Cherukuri, H. P., and T. G. Shawki	An energy-based localization theory: Part II—Effects of the diffusion, inertia and dissipation numbers	Aug. 1993
720	Aref, H., and S. W. Jones	Chaotic motion of a solid through ideal fluid	Aug. 1993
721	Stewart, D. S.	Lectures on detonation physics: Introduction to the theory of detonation shock dynamics	Aug. 1993
722	Lawrence, C. J., and R. Mei	Long-time behavior of the drag on a body in impulsive motion	Sept. 1993
723	Mei, R., J. F. Klausner, and C. J. Lawrence	A note on the history force on a spherical bubble at finite Reynolds number	Sept. 1993
724	Qi, Q., R. E. Johnson, and J. G. Harris	A re-examination of the boundary layer attenuation and acoustic streaming accompanying plane wave propagation in a circular tube	Sept. 1993
725	Turner, J. A., and R. L. Weaver	Radiative transfer of ultrasound	Sept. 1993
726	Yogeswaren, E. K., and J. G. Harris	A model of a confocal ultrasonic inspection system for interfaces	Sept. 1993
727	Yao, J., and D. S. Stewart	On the normal detonation shock velocity–curvature relationship for materials with large activation energy	Sept. 1993
728	Qi, Q.	Attenuated leaky Rayleigh waves	Oct. 1993
729	Sofronis, P., and H. K. Birnbaum	Mechanics of hydrogen–dislocation–impurity interactions: Part I—Increasing shear modulus	Oct. 1993
730	Hsia, K. J., Z. Suo, and W. Yang	Cleavage due to dislocation confinement in layered materials	Oct. 1993
731	Acharya, A., and T. G. Shawki	A second-deformation-gradient theory of plasticity	Oct. 1993
732	Michaleris, P., D. A. Tortorelli, and C. A. Vidal	Tangent operators and design sensitivity formulations for transient nonlinear coupled problems with applications to elasto-plasticity	Nov. 1993
733	Michaleris, P., D. A. Tortorelli, and C. A. Vidal	Analysis and optimization of weakly coupled thermo-elasto-plastic systems with applications to weldment design	Nov. 1993

(continued)

List of Recent TAM Reports (cont'd)

No.	*Authors*	*Title*	*Date*
734	Ford, D. K., and D. S. Stewart	Probabilistic modeling of propellant beds exposed to strong stimulus	Nov. 1993
735	Mei, R., R. J. Adrian, and T. J. Hanratty	Particle dispersion in isotropic turbulence under the influence of non-Stokesian drag and gravitational settling	Nov. 1993
736	Dey, N., D. F. Socie, and K. J. Hsia	Static and cyclic fatigue failure at high temperature in ceramics containing grain boundary viscous phase: Part I—Experiments	Nov. 1993
737	Dey, N., D. F. Socie, and K. J. Hsia	Static and cyclic fatigue failure at high temperature in ceramics containing grain boundary viscous phase: Part II—Modelling	Nov. 1993
738	Turner, J. A., and R. L. Weaver	Radiative transfer and multiple scattering of diffuse ultrasound in polycrystalline media	Nov. 1993
739	Qi, Q., and R. E. Johnson	Resin flows through a porous fiber collection in pultrusion processing	Dec. 1993
740	Weaver, R. L., W. Sachse, and K. Y. Kim	Transient elastic waves in a transversely isotropic plate	Dec. 1993
741	Zhang, Y., and R. L. Weaver	Scattering from a thin random fluid layer	Dec. 1993
742	Weaver, R. L., and W. Sachse	Diffusion of ultrasound in a glass bead slurry	Dec. 1993
743	Sundermeyer, J. N., and R. L. Weaver	On crack identification and characterization in a beam by nonlinear vibration analysis	Dec. 1993
744	Li, L., and N. R. Sottos	Predictions of static displacements in 1–3 piezocomposites	Dec. 1993
745	Jones, S. W.	Chaotic advection and dispersion	Jan. 1994
746	Stewart, D. S., and J. Yao	Critical detonation shock curvature and failure dynamics: Developments in the theory of detonation shock dynamics	Feb. 1994
747	Mei, R., and R. J. Adrian	Effect of Reynolds-number-dependent turbulence structure on the dispersion of fluid and particles	Feb. 1994
748	Liu, Z.-C., R. J. Adrian, and T. J. Hanratty	Reynolds-number similarity of orthogonal decomposition of the outer layer of turbulent wall flow	Feb. 1994